Hindawi
Advances in Civil Engineering
Volume 2023, Article ID 6668963, 21 pages
https://doi.org/10.1155/2023/6668963

*Research Article*

# Evaluation of Rutting, Fatigue, and Moisture Resistance of Low-Energy Asphalt Mixtures Modified by Crumb Rubber

**Saeid Moghimi,[1] Gholamali Shafabakhsh ,[1] and Hassan Divandari[2]**

[1]*Department of Highway and Transportation Engineering, Faculty of Civil Engineering, Semnan University, Semnan, Iran*
[2]*Department of Civil Engineering, Central Tehran Branch, Islamic Azad University, Tehran, Iran*

Correspondence should be addressed to Gholamali Shafabakhsh; ghshafabakhsh@semnan.ac.ir

Received 23 November 2022; Revised 5 May 2023; Accepted 25 August 2023; Published 5 October 2023

Academic Editor: Giulio Dondi



Low-energy asphalt (LEA) mixture, as an alternative to hot mix asphalt (HMA) due to its lower mixing temperature, has advantages such as reducing energy consumption and environmental pollutants. LEA has poor performance characteristics due to the presence of water in its manufacturing process and low mixing temperature. All the studies about LEA have been focused only on investigating the performance of this asphalt mixture, and the effect of additives in its modification is one of the research gaps in this field. Therefore, the use of crumb rubber (CR) and determining its optimal percentage in modifying the performance characteristics of LEA is considered an innovation of this research. In this research, the performance characteristics of LEA modified by 10%, 15%, and 20% CR were evaluated. In order to examine the rutting behavior, moisture sensitivity and fatigue resistance, dynamic creep, indirect tensile strength (ITS), and four-point bending beam tests were applied, respectively. The results of creep curves and flow numbers (FNs) indicated that modifying LEA by 15% increased the rutting resistance by 1.92 and 2.3 times, respectively, compared to the HMA specimen at the stress level of 207 and 310 kPa. Moreover, the evaluation of the creep strain slope revealed that modifying LEA significantly reduced stress sensitivity. ITS test showed an increase in tensile strength ratio by 22% in the specimen with 10% CR compared to the unmodified specimen. In the evaluation of fatigue resistance, while LEA containing 10% CR had almost similar results to the HMA specimen, other specimens represented a shorter fatigue life, so that with the increase in CR percentage, the fatigue life decreased. Determination of fatigue life by energy ratio and Rowe and Bouldin criteria showed similar results. Finally, by determining the plateau value (PV) in the ratio of the dissipated energy change method, the lowest PV was assigned to the 10% CR-modified LEA and HMA specimens, respectively.

## 1. Introduction

The occurrence of the industrial revolution and the development of technology have resulted in many environmental pollutions that threaten human societies [1, 2]. Currently, the indiscriminate emission of greenhouse gases and global warming has caused many changes in the climate system, which can have irreparable consequences [3–6]. Today, there are cost-effective solutions that will lead the global community toward a cleaner and safer economy to promote sustainable development [7, 8]. One of these solutions is to find alternatives for producing hot mix asphalt (HMA) [9]. HMA consists of a mixture of aggregates and asphalt binder at temperatures above 160°C, which is associated with high consumption of fossil fuels and emission of CO, $SO_2$, $CO_2$, and $NO_x$ due to the high production temperature. These negative environmental effects will result in global warming [10]. In recent years, many efforts have been made to develop asphalt mixtures using green technologies, which have decreased the negative points of HMA by reducing its temperature during production and compaction [11, 12]. One of these measures is the production of low-energy asphalt (LEA), which is a component of half-warm mix asphalt with a temperature range of 80–100°C [13].

LEA technology was first developed in 2006 by LEA-CO in France. The construction of this asphalt is based on following a sequential process so that the aggregates are initially divided into two sections: coarse and fine aggregates. Coarse aggregates, like HMA, are heated to 170°C and then mixed with a hot asphalt binder. After creating a suitable coating for

asphalt binder and coarse aggregates, fine aggregates are added to the mixture in a moist form at room temperature [14]. The addition of fine aggregates and the moisture in it when faced with coarse aggregates and asphalt binder causes the formation of foam in the mixture and reduces asphalt binder viscosity [15]. On the other hand, after the wet fine aggregates come into contact with the bituminous coarse aggregates, the air trapped between the asphalt binder and water is sufficiently heated and turns water vapor into foam. However, since this occurs under normal conditions at temperatures under 100°C, the final temperature of the mixture should ideally be less than 100°C. Among the important benefits of this asphalt is its significant saving in energy consumption, which is because only coarse aggregates need a temperature higher than 100°C to create a bituminous coating, and no energy is needed to heat and dry fine aggregates [16]. Also, the low temperature of this mixture during mixing minimizes the production of greenhouse gases and the emission of volatile substances caused by heating the asphalt binder, so this mixture is compatible with the environment and nature [17]. In addition, the formation of foam and consequently the reduction of asphalt binder viscosity and the softness of the mixture due to the reduction of asphalt binder aging are among the factors that increase its compaction [18]. Increasing the safety factor for workers during execution due to the low temperature and less need for solvents to wash and clean the equipment at the end of daily operations are other benefits of using this mixture [19].

One of the most important studies on the characteristics of LEA and its comparison with other asphalt mixtures is the research presented in the NCHRP 9-43 project report. To evaluate the performance properties, asphalt mixtures such as LEA, HMA, and two types of hot asphalt mixtures modified by advera and sasobit, respectively, were made in an equal percentage of air void and evaluated by conducting several tests. According to the results obtained from the dynamic creep test, the highest rutting resistance was recorded for the sasobit-modified specimen, and the lowest value was for the LEA specimen. In this evaluation, the HMA specimen with a flow number (FN) of about two times compared to the LEA specimen was more favorable. Also, according to the moisture sensitivity results, LEA, with the highest tensile strength ratio (TSR), was the most resistant specimen compared to other mixtures. The reason for this was the use of an antistripping agent in constructing LEA. Also, the dynamic modulus test was applied to determine the viscoelastic properties of asphalt mixtures, which showed the lowest dynamic modulus in all frequency and temperature ranges for the LEA specimen. The lower stiffness of the mixture and its softness compared to other specimens due to the lower mix temperature and less aging in the manufacturing process were reported as the reason for the low dynamic modulus for this asphalt [20].

Harder et al. [16] conducted a laboratory and field study of the mechanical and environmental characteristics of LEA. At first, it was found that the residual moisture in the specimen has a great role in the compactibility and workability of the LEA specimen, so that the LEA specimen was compacted in a lower percentage of air voids and the number of gyrations. Also, to determine the viscoelastic properties of LEA, the dynamic modulus test according to NCHRP 9-29 was performed at three temperatures and four different frequencies. The results showed a decrease in the dynamic modulus of LEA specimens compared to HMA, which was reported due to less aging and consequently less stiffness of asphalt binder during the production of mixtures. In addition, the evaluation of energy consumption for manufacturing LEA showed a reduction of about 33% compared to HMA. Another part of this study was the evaluation of LEA pollution potential. The results showed that LEA production reduced particulate matter by 51%, nitrogen oxide by 21%, and carbon monoxide by 82%. Also, the concentration of sulfur oxide decreased by 46%. Other contaminants during asphalt production include formaldehyde. Moreover, it was found that in the manufacturing process of LEA, the production of this material was significantly reduced by 95% compared to the HMA specimen [21]. Carter et al. [19] examined the compactibility of LEA and compared it with HMA and Evothem and Sasobit-modified warm mix asphalts. In this study, specimens were compacted by the Superpave gyratory compactor, and the number of gyrations was evaluated in terms of their air void percentage. According to the results, while LEA and the specimens containing Sasobit showed the best performance, the specimen containing Evotherm was the most incompactible specimen [19]. In another study, Olard and Gaudefroy compared the functional and environmental properties of LEA, including compressive strength, moisture resistance, complex modulus, and fatigue resistance. In this regard, LEA specimens were prepared and evaluated by several tests. The results of the moisture resistance test showed that LEA had a lower moisture resistance than the control specimen. Also, the values of the complex modulus obtained in the dynamic modulus test indicated a higher value of this parameter for HMA, which was due to the lower aging of the asphalt binder caused by the lower mixing temperature in the LEA fabrication process. Finally, the results of the fatigue resistance test showed shorter fatigue life and lower fatigue resistance of LEA [22]. Some et al. [23] evaluated the mechanical properties of LEA, including complex modulus, fatigue resistance, and moisture sensitivity. The complex modulus determination test was performed according to EN 12697-26, and the results showed almost the same dynamic modulus at 15°C and 5 Hz frequency for LEA and HMA. Moreover, the results of the fatigue test represented lower fatigue resistance of LEA compared to HMA. Evaluation of moisture sensitivity of asphalt mixtures also indicated lower moisture resistance of LEA compared to HMA [23]. Zelelew et al. [24] examined the rutting, fatigue, and moisture resistance of unmodified LEA mixtures and compared the results with modified HMA by sasobit, advera, and gencor. In this regard, by performing the Humburg wheel track test, the number of wheel crossings to develop the rut with a depth of 20 mm was determined. In this evaluation, the highest number of crossings was assigned to the LEA specimen, followed by the HMA specimen. Also, determining the moisture sensitivity of asphalt mixtures using this test was one of the other evaluation items in

Table 1: Specifications of limestone aggregates.

| Properties | | Standard | Results | | |
|---|---|---|---|---|---|
| | | | Coarse aggregate | Fine aggregate | Filler |
| Sand equivalent (%) | | AASHTO-T176 | – | 69 | – |
| Los Angeles abrasion loss (%) | | AASHTO-T96 | 17 | – | – |
| Atterberg limits | PI | ASTM-D4318 | – | Nonplastic | Nonplastic |
| | PL | | – | – | – |
| | LL | | – | Indeterminate | Indeterminate |
| Percentage of fractured particles (%) | | ASTM-D5821 | 100 | – | – |
| Boiling water (%) | | ASTM-D3625 | <5 | – | – |
| Soundness (5 cycles), sodium sulfate (%) | | AASHTO-T104 | 1 | 3 | – |

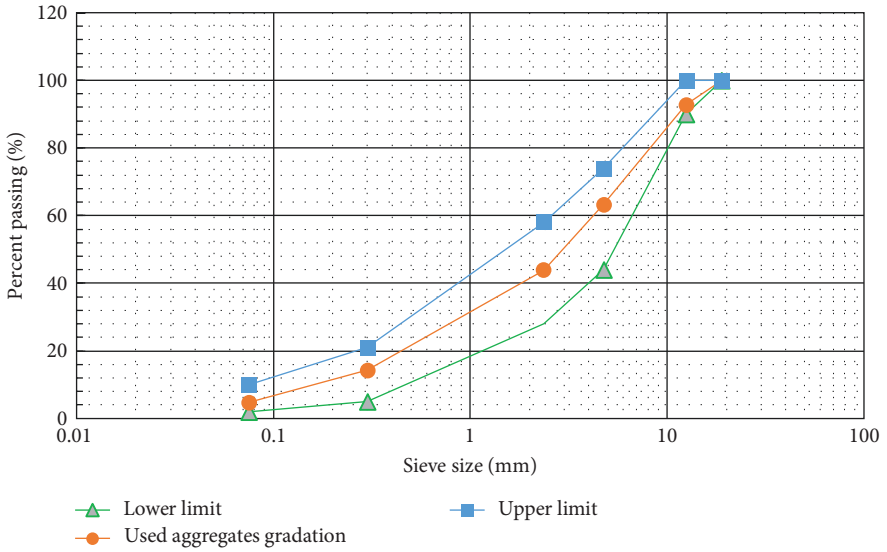


Figure 1: Gradation curve.

this study, which was specified by determining indicators such as Humburg stripping slope and Humburg inflection point. Although LEA had lower moisture resistance than HMA and sasobit-modified specimens, it was much more resistant than the Advera and Gencor specimens. Another item evaluated in this study was determining FN for asphalt mixtures. According to the results, the highest value of FN was associated with the LEA specimen due to the lower percentage of asphalt binder in the construction process compared to other asphalt mixtures. The last evaluation in this study was to specify the fatigue resistance index by determining the stiffness and phase angle values at 21°C and 5 Hz frequency using the dynamic modulus test. The results of this study showed the lowest fatigue resistance for LEA specimen [24].

According to previous studies, researchers have focused on the different performances of LEA compared to HMA. However, the influence of crumb rubber (CR) on the rutting, fatigue, and moisture performance of LEA has not been investigated so far. Also, for the first time, the fatigue resistance of LEA was investigated by the four-point bending beam method. Therefore, the use of CR and determining its optimal percentage in modifying the performance characteristics of LEA was an innovation of this study to improve the asphalt binder and cover all its weaknesses. In this regard, HMA and LEA specimens without the additive were used as control specimens to compare the effect of 10%, 15%, and 20% CR additive on LEA and determine the optimal percentage of CR. The dynamic creep test was used to evaluate the rutting resistance of this asphalt. Also, the four-point beam fatigue test and modified Lottman test were used to evaluate the fatigue and moisture resistances of asphalt mixtures.

## 2. Materials and Methods

*2.1. Materials.* In this study, limestone aggregates were used to make LEA mixtures. Table 1 provides the specifications of applied aggregates. Also, Figure 1 presents the gradation of aggregates. To fabricate asphalt mixtures, asphalt binder with 60/70 penetration grade was used, the physical characteristics of which are presented in Table 2.

*2.2. Additive.* CR additive was used in this research to improve the performance of LEA. During the process of

Table 2: Specifications of base binder.

| Properties | Standard | Results |
|---|---|---|
| Specific gravity at 25°C (g/cm$^3$) | ASTM-D70 | 1.016 |
| Penetration at 25°C (0.1 mm) | ASTM-D6 | 63 |
| Softening point (°C) | ASTM-D36 | 49.2 |
| Flashpoint (°C) | ASTM-D92 | 305 |
| Kinematic viscosity at 120°C (cSt) | | 773 |
| Kinematic viscosity at 135°C (cSt) | ASTM-D2170 | 342 |
| Kinematic viscosity at 160°C (cSt) | | 141 |
| Heating loss (%) | ASTM-D1754 | 0.22 |

Table 3: Specifications of CR.

| Physical | | Chemical | | |
|---|---|---|---|---|
| Moisture (%) | Density (g/cm$^3$) | Acetone extractive (%) | Ash (%) | Rubber hydrocarbon (%) |
| 0.43 | 1.15 | 19 | 7.6 | 48 |

Table 4: CR gradation.

| Percent passing (%) | Sieve size (mm) |
|---|---|
| 100 | No. 30 (850 $\mu$m) |
| 89 | No. 40 (600 $\mu$m) |
| 57.7 | No. 50 (425 $\mu$m) |
| 23 | No. 80 (300 $\mu$m) |
| 18.3 | No. 100 (150 $\mu$m) |

urbanization and construction [25–28], a significant amount of waste materials is generated, including waste tires. Considering the growing concern of human society in the accumulation of waste, CR was the best choice to improve LEA specifications, the use of which was in line with the environmental and economic goals of fabricating this type of asphalt mixture. Also, according to the research conducted on this additive and its significant effect on the performance characteristics of asphalt binder and mixture in the range of 10%–20% by weight of the binder, in this research, CR was used in 10%, 15%, and 20% [29]. Table 3 shows the physical and chemical specifications of CR applied in this research.

In this study, CR produced by ambient grinding with smaller particles and powder with mesh size 40 was utilized according to the gradation presented in Table 4. Also, according to previous research, to achieve a homogeneous mixture and the best performance conditions, the asphalt binder temperature during mixing was selected to be 180°C, and a high shear mixer with 2,000 rpm was used for 2 hr [30]. Table 5 presents the properties of CR-modified asphalt binder.

In this study, according to the economic goals in the production of LEA and its competitiveness in the production of HMA, stabilizer additives were not used in the asphalt binder modification process. Therefore, in order to eliminate the concern of CR instability in the asphalt binder, while performing storage stability evaluation, the modified asphalt binder was used immediately after production to manufacture asphalt mixtures. According to Table 6, the storage stability evaluation based on AASHTO P-55 for modified binders was conducted by performing the softening point test from the top and bottom of the specimens in an aluminum tube. As the results show, although the difference in softening point increases with the increase in the percentage of CR, the values obtained are less than 2.5°C, which is defined as the maximum specification in this standard.

*2.3. Mix Design.* In this study, the guidelines presented in NCHRP Report 691 were used as criteria for producing LEA specimens. In this regard, the Superpave volumetric mix design was used according to AASHTO R35. One of the important factors in fabricating LEA is the maximum size of fine aggregates, and the studies on this asphalt show that this factor is limited to 2–3 mm [17, 18, 21, 22, 24]. Therefore, in this study, sieve no. 8 was used as a separator for coarse and fine aggregates. According to NCHRP Report 691, the moisture content of fine aggregates is suggested to be between 3% and 4% by weight. Also, to ensure the drying of coarse aggregates, these materials were placed in an oven for 4 hr at 170°C, and fine aggregates were used without heating at room temperature. Another point in producing LEA is choosing the temperature of the asphalt binder. According to the report, this temperature is limited to 130°C [20]. In this study, in order to fabricate LEA specimens according to NCHRP Report 09-43, coarse aggregates and asphalt binder were first heated to 170 and 130°C, respectively. Then, coarse aggregates were mixed with asphalt binder in a wire mixer, and after at least 30 s and ensuring full coverage of the obtained mixture, wet fine aggregates with a moisture content of 3.5% by weight were added to the mixture. The contact of moisture with hot asphalt binder caused the formation of foam, according to Figure 2, and after that, mixing operations continued until the complete coating of fine aggregates. Also, due to the necessity of placing the temperature range of LEA in the range of 80–100°C, as well as its half-warm nature and the effect of this temperature on

Table 5: Properties of CR modified binder.

| Binder property | Standard | Unit | CR percentage | | | |
|---|---|---|---|---|---|---|
| | | | 0 | 10 | 15 | 20 |
| Penetration at 25°C | ASTM-D5 | 0.1 mm | 63 | 47 | 43 | 34 |
| Softening point | ASTM-D36 | °C | 49.2 | 58.3 | 61 | 73.1 |
| Viscosity at 135°C | ASTM-D2170 | cST | 342 | 717 | 824 | 1,218 |
| Specific gravity | ASTM-D70 | g/cm$^3$ | 1.016 | 1.037 | 1.041 | 1.049 |

Table 6: Storage stability test for modified binders.

| CR percentage | Softening point (°C) | | $S(b)$–$S(t)$ |
|---|---|---|---|
| | Top | Bottom | |
| 10 | 57.8 | 59.3 | 1.5 |
| 15 | 60.3 | 62.2 | 1.9 |
| 20 | 71.7 | 74.1 | 2.4 |

Figure 2: Created foam in LEA.

reducing energy consumption and compaction of asphalt, the mixing temperature was recorded after each step of the mixing operation. After mixing asphalt binder with aggregates, the specimens were compacted using a gyratory compaction device based on AASHTO T 312. In order to determine the optimum bitumen content (OBC), the necessary tests were performed on compacted and noncompacted specimens, and the volume characteristics of mixtures, their OBC, and the final mixing temperature were recorded for each of the mentioned specimens according to Table 7.

### 2.4. Experimental Program

*2.4.1. Moisture Sensitivity.* The most common method for evaluating the moisture sensitivity of asphalt mixtures is the modified Lottman test according to AASHTO T 283, in which a criterion for evaluating the effect of water on the asphalt mixture and its moisture sensitivity is specified by determining the ratio of indirect tensile strength (ITS) of unconditioned specimens to the conditioned ones [31]. Unconditioned specimens are tested by placing them in a water bath at 25°C for 30–40 min, and conditioned specimens, after obtaining 70%–80% saturation and being placed at −18°C for 16 hr, are kept in a water bath with a temperature of 60°C for 24 hr. The specimens were tested three times with a loading rate of 50 mm/min at a temperature of 25°C and ITS ($S_t$) in kPa was determined by Equation (1), where $P$ is the maximum load ($N$), t is the specimen thickness (mm), and $D$ is the specimen diameter (mm). Also, the TSR is determined according to Equation (2), where $S_1$ and $S_2$ are ITS values for unconditioned and conditioned specimens (kPa), respectively [32–34].

$$S_t = \frac{2,000P}{\pi t D}. \tag{1}$$

$$\text{TSR} = \frac{S_2}{S_1}. \tag{2}$$

*2.4.2. Dynamic Creep Test.* In this research, the dynamic creep test was performed using a universal testing machine according to AASHTO T 378 to determine permanent deformations. This test is performed by applying repetitive axial stress to specimens, and the deformation in each load cycle is determined by linear variable differential transducers (LVDTs). The strain of asphalt specimens is then calculated by Equation (3), where $\varepsilon$ is the accumulated strain, $h$ is the axial deformation (mm), and $H_\circ$ is the initial specimen height (mm). Finally, a creep curve is drawn to evaluate mixtures against rutting [35].

$$\varepsilon = \frac{h}{H_\circ}. \tag{3}$$

The creep curve is an ascending accumulated strain graph consisting of three zones. During the first zone, as the number of load cycles increases, the strain rate in asphalt mixtures decreases steadily. In the second zone, the strain experiences a constant rate, and finally, the strain rate grows increasingly during the third zone [36]. To determine the strain behavior of asphalt mixtures versus the load cycle, Zhou et al. presented a three-stage model as follows, which has been used by many researchers due to its high modeling ability [37, 38].

Table 7: Volumetric properties of asphalt mixtures.

| Volumetric properties | Gmm | Gmb | Va (%) | VMA (%) | VFA (%) | OBC (%) | Mix temperature (°C) |
|---|---|---|---|---|---|---|---|
| HMA | 2.449 | 2.353 | 3.92 | 14.97 | 73.82 | 4.6 | 160 |
| LEA | 2.466 | 2.368 | 3.97 | 14.24 | 72.14 | 4.4 | 90 |
| LEA + 10% CR | 2.447 | 2.351 | 4.01 | 15.06 | 73.37 | 4.6 | 92 |
| LEA + 15% CR | 2.449 | 2.353 | 3.93 | 15.16 | 74.05 | 4.8 | 92 |
| LEA + 20% CR | 2.451 | 2.354 | 3.94 | 15.45 | 74.05 | 5.2 | 98 |

$$\begin{aligned}
&\text{Primary stage: } \varepsilon_p = aN^b.N < N_{\text{ps}},\\
&\text{Secondary stage: } \varepsilon_P = \varepsilon_{\text{PS}} + c(N - N_{\text{PS}}).\varepsilon_{\text{PS}}\\
&\qquad = aN_{\text{PS}}^b.N_{\text{PS}} \le N \le N_{\text{ST}},\\
&\text{Tertiary stage: } \varepsilon_P = \varepsilon_{\text{ST}} + d\left(e^{f(N-N_{\text{ST}})} - 1\right).\varepsilon_{\text{ST}}\\
&\qquad = \varepsilon_{\text{PS}} + c(N_{\text{ST}} - N_{\text{PS}}),\ N \ge N_{\text{ST}},
\end{aligned} \tag{4}$$

where $a$, $b$, $c$, $d$, and $f$ are material constants, $\varepsilon_P$ is plastic strain, $N$ is the number of cycles, $N_{\text{PS}}$ is the number of cycles at the beginning of the secondary stage, $N_{\text{ST}}$ is the number of cycles at the beginning of the tertiary stage, $\varepsilon_{\text{PS}}$ is the accumulated plastic strain at the beginning of the secondary region, and $\varepsilon_{\text{ST}}$ is the accumulated plastic strain at the beginning of the tertiary stage.

In this study, according to the proposed standard, cylindrical specimens with a diameter of 100 mm and a height of 150 mm were made. Then, each specimen was placed in a temperature-controlled cabinet at 54°C for 2 hr to achieve temperature equilibrium. Given the fact that rutting failure occurs at the beginning of the service life of asphalt mixtures in conditions where the pavement may not have reached the final density, the air void of specimens in this experiment was considered to be 7%. Also, since the traffic load has an influence on the fatigue life, in order to investigate the effect of traffic intensity, the experiment was performed at two stress levels of 207 and 310 kPa, and loading and rest times after each load cycle were selected as 0.1 and 0.9 s, respectively. This experiment was repeated three times for each type of asphalt mixture, and the average of the obtained results was used to draw creep curves.

*2.4.3. Four-Point Beam Fatigue Test.* The four-point beam fatigue test was performed according to AASHTO T321 by constant strain method, and a semi-sinusoidal load with a frequency of 10 Hz was applied to the specimens at two strain levels of 400 and 700 $\varepsilon\mu$. Since the occurrence of fatigue cracks at ambient temperature is the most common, in this study, the beam fatigue test was performed at 22°C and repeated three times for each mixture type of asphalt mixture. The asphalt slabs were made by roller compactor in a 4% air void, and finally, specimens were created in dimensions of $380 \times 60 \times 50$ mm. Equations (5) and (6) calculate the output parameters, where $\sigma_t$ is the maximum tensile stress (Pa), $P$ is the applied load (N), $b$ is the specimen width (m), $\varepsilon_t$ is the maximum tensile strain ($\varepsilon\mu$), $\delta$ is the maximum intermediate deformation of the beam (m), $a$ is the distance between the middle frame clamps (m), and $L$ is the distance between the outer clamps and the supports (m).

$$\sigma_t = 0.357\frac{P}{bh^2}. \tag{5}$$

$$\varepsilon_t = \frac{12\delta h}{3L^2 - 4a^2}. \tag{6}$$

By calculating the maximum tensile stress and strain, flexural stiffness is determined by Equation (7), where $S_t$ is the maximum flexural stiffness (Pa).

$$S_t = \frac{\sigma_t}{\varepsilon_t}. \tag{7}$$

To determine the fatigue life of specimens, three methods are used as follows. The first method is known as the classical failure criterion, in which fatigue life ($N_{f50}$) refers to the number of load cycles equivalent to a 50% reduction in stiffness modulus. According to AASHTT T321-14, the initial stiffness modulus is flexural stiffness in the 50th cycle. In this method, it is assumed that macrocracks begin to appear when the initial stiffness modulus reaches 50% of its value. The second method is based on dissipated energy, according to which the fatigue life is related to the dissipated energy. In this method, several ways are defined to determine the fatigue life of asphalt mixtures. The third method is called failure mechanics. Unlike the second method, the failure mechanics calculate the fatigue life of asphalt mixtures based on the residual energy [39, 40].

The dissipated energy method is a suitable criterion for evaluating fatigue failure due to its simplicity in determining various parameters. In this method, the dissipated energy in each load cycle is determined using Equation (8), where $W_i$ is the dissipated energy (Pa) in the ith cycle and $\varepsilon_i$, $S_i$, $\varphi_i$ are strain ($\mu\varepsilon$), flexural stiffness (Pa), and angle in the ith cycle (degree), respectively.

$$W_i = \pi\varepsilon_i^2 S_i \sin\varphi_i. \tag{8}$$

Based on the dissipated energy method, many criteria have been presented to determine the initiation of cracks. One of these methods is energy ratio according to Equation (9), provided by Pronk and Hopman [41], where $W_1$ is the initial dissipated energy (IDE), n is the number of load cycles, and $W_n$ represents the dissipated energy in the nth cycle.

$$\mathrm{ER} = \frac{n \times W_1}{W_n}. \tag{9}$$

In this method, the onset of macro fatigue failures occurs at a point ($N_{\mathrm{ER}}$), where the energy ratio curve deviates from the tangent line compared to the load cycle curve. Since the determination of this point is done by fitting the diagram and engineering judgment, this method is not a reliable method to evaluate the fatigue failure of asphalt mixtures. Therefore, Rowe and Bouldin, by defining the product of stiffness in the number of load cycles ($S_i \times n_i$), presented another criterion to determine the failure [39], where $S_i$ is the flexural stiffness (kPa) and $n_i$ is the number of load cycles. In this method, the failure point ($N_{S\times n}$) occurs when the $S \times n$ curve reaches its maximum value according to the load cycle. In this situation, the microcracks are transformed into macrocracks by changing their form [42].

Another criterion for assessing fatigue failure is to determine the parameters of IDE and cumulative dissipated energy (CDE). IDE refers to the energy lost in the 50th cycle. CDE is the sum of dissipated energies from the first to the nth cycle, which is calculated according to Equation (10).

$$\mathrm{CDE} = \sum_{i=1}^{n} \mathrm{DE}_i, \tag{10}$$

where CDE is the cumulative dissipated energy (Pa) and $\mathrm{DE}_i$ is the energy dissipated in the ith cycle (Pa). Since these relationships are highly influenced by the type of materials and test conditions, their use as a criterion for assessing fatigue failure is not reliable [43]. Therefore, in order to eliminate the mentioned weaknesses, the criterion of the dissipated energy change (RDEC) ratio was defined according to Equation (11) to identify the correct point of failure:

$$\mathrm{RDEC} = \frac{\mathrm{DE}_{n+1} - \mathrm{DE}_n}{\mathrm{DE}_n}, \tag{11}$$

where $\mathrm{DE}_n$ and $\mathrm{DE}_{n+1}$ are the dissipated energy in the $n$ and $n+1$ cycles, respectively. The procedure of the research method is represented in Figure 3.

## 3. Results and Discussion

*3.1. Dynamic Creep.* The results of the dynamic creep test are presented in Figures 4 and 5, which represent accumulated strain diagrams versus the number of load cycles at the stress level of 207 and 310 kPa, respectively. As can be seen, there are significant differences between these graphs for different specimens, indicating the difference in their creep behavior. Also, the occurrence of all three creep regions in all diagrams confirms the correct choice of 2,200 final load cycles in this test.

In general, lower values of accumulated strain indicate higher resistance of asphalt mixtures to permanent deformations and their low potential against rutting. As can be seen in Figures 4 and 5, LEA specimens modified by CR have the best performance against rutting, which is not only true for LEA specimens containing 20% CR. The low values of accumulated strain for LEA specimens containing 15% and 10% CR are due to the fact that the dissolution of part of CR inside the asphalt binder causes the aromatic oils of the asphalt binder to be absorbed by the rubber polymer chains; as a result, the asphalt binder changes to a gel-like form and increases its viscosity and elasticity. An increase in viscosity leads to an increase in the asphalt binder film on the aggregates and their better connection and ultimately results in an increase in the strength of the mixture. In addition, the unresolved part of CR also plays a key role in increasing the strength of the mixture so that these particles, while maintaining their integrity together, form a 3D network that this amplifying network can be effective against the spread of permanent deformations [38]. On the other hand, by looking at the creep curve and comparing the strain values, it is clear that the modified LEA specimen with 20% additive has more accumulated strain compared to other modified specimens and even HMA specimens. By increasing CR to the mentioned value, the amount of absorbed light oils in the asphalt binder is increased, and the viscosity of asphalt binder increases excessively, which has a negative effect on the ability of asphalt binder to better cover the aggregates and reduces the integrity and cohesion of the mixture and, as a result, its strength and stiffness. Another effective factor in the low rutting resistance of the specimen modified by 20% CR is the low-mixing temperature of asphalt binder and aggregates for this mixture. The need to set the mixing temperature in LEA specimens in the range of 80–100°C means that the modified asphalt binder does not have the ability to properly cover the aggregates due to its high viscosity. Therefore, this specimen does not have the desired strength and rigidity. Therefore, in order to achieve a more suitable mixture of asphalt binder and aggregate, a higher temperature is required for the mentioned specimen. Also, the high strain values in the unmodified LEA specimen are due to the low-mixing temperature, and as a result, less asphalt binder aging than HMA. The lower viscosity of the asphalt binder leads to softening of the mixture, leading to less stiffness of this asphalt mixture compared to others.

In addition, the investigation of the number of load cycles at 1% strain indicates a significant increase in the number of load cycles for LEA specimens with 15% and 10% CR compared to other specimens. According to Figure 6, this increase at the stress of 207 kPa for these specimens is 3.9 and 1.2 times higher than HMA as well as 12.5 and 6.1 times higher than LEA specimens, respectively. Similarly, evaluating this parameter at the stress of 310 kPa shows an increase of 3.9 and 2.2 times compared to HMA as well as 7.3 and 4.2 times increases compared to the unmodified LEA. As is evident, the other three specimens follow a similar trend at both strain levels, and the negative effect of increasing CR to 20% in degrading the rutting resistance and lower load cycles in the mentioned strain compared to HMA is quite obvious. Also, in this comparison, the lowest number of load cycles at strains 207 and 310 belong to the unmodified LEA.

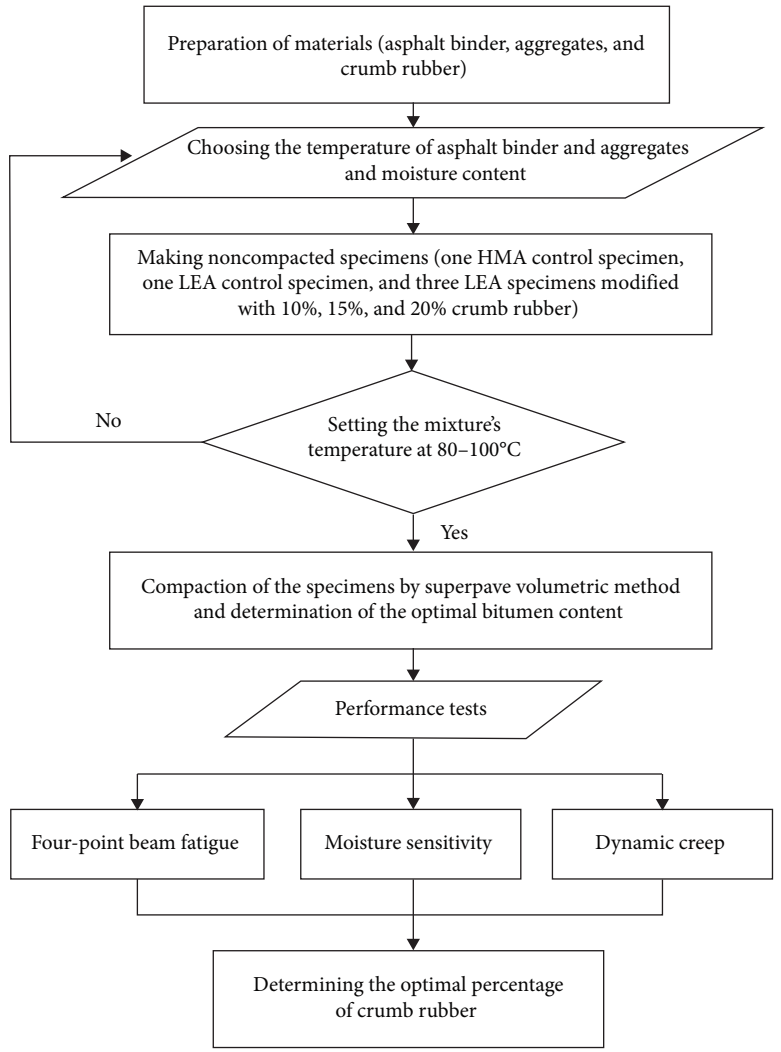


Figure 3: Steps of the research method.

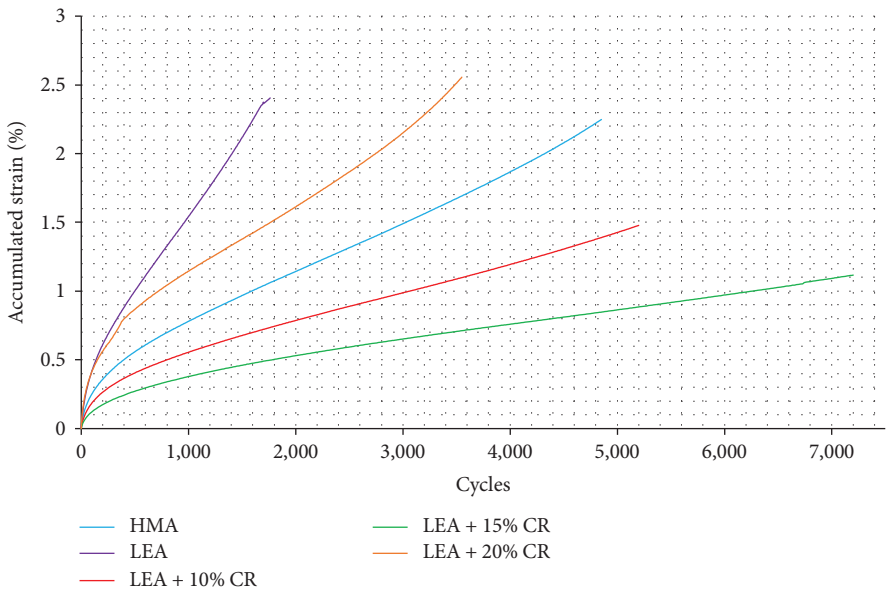


Figure 4: Accumulated strain versus load cycle for asphalt mixtures at 207 kPa.

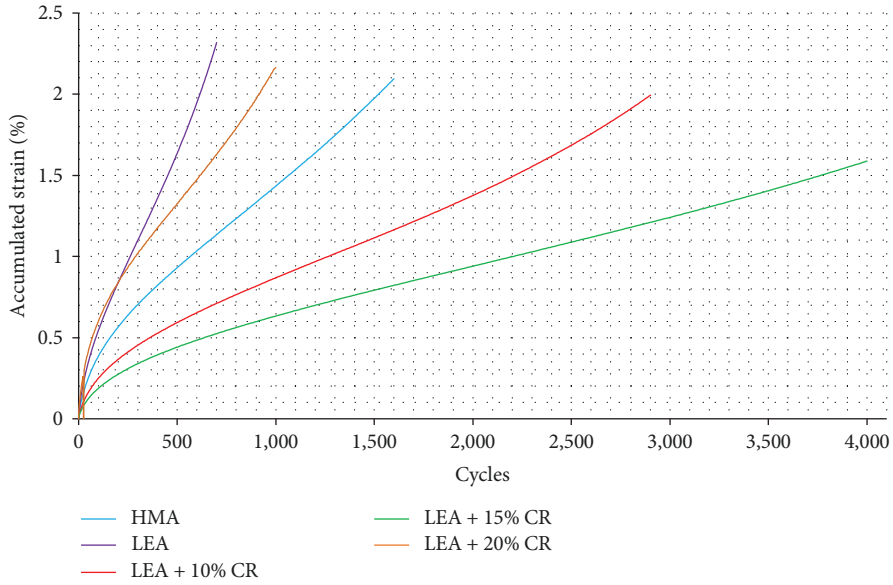


Figure 5: Accumulated strain versus load cycle for asphalt mixtures at 310 kPa.

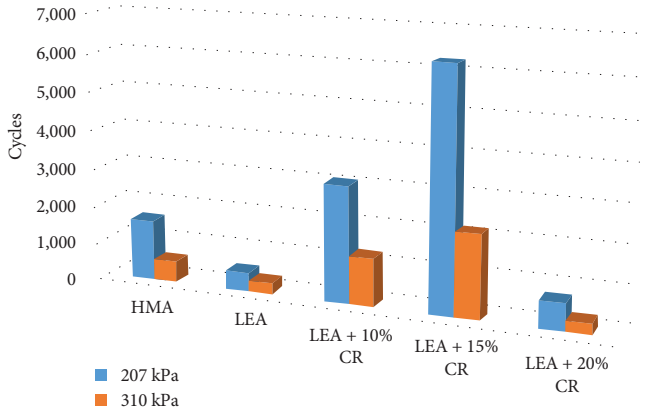


Figure 6: Number of load cycles at 1% strain.

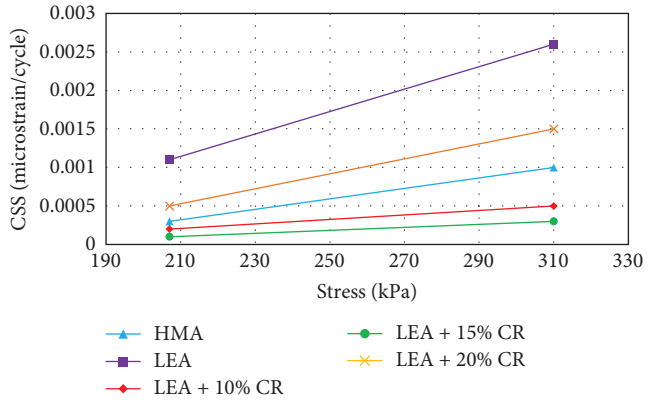


Figure 7: CSS results for asphalt mixtures versus stress levels.

Creep strain slope (CSS) is one of the other effective parameters in assessing permanent deformations. CSS is the slope of the second zone of the creep curve, which indicates the developing rate of deformation. In the condition that the loading stress is constant, this slope will have an almost constant value that can be measured through linear regression [44]. Figures 7 and 8 show CSS results and the variation rate for LEA and control specimens. As the results show, increasing the stress level increased CSS values for all tested specimens. In this evaluation, the highest rate of CSS changes is related to LEA specimens without the additive, and the lowest amount is associated with 15% and 10% CR-modified LEA specimens, respectively. For example, with an increase in stress from 207 to 310 kPa, the rate of these changes for LEA specimens without the additive is 7.5 and 5 times higher than the modified LEA specimens containing 15% and 10% CR, respectively. Therefore, it is very important to state that the modification of LEA specimens by CR

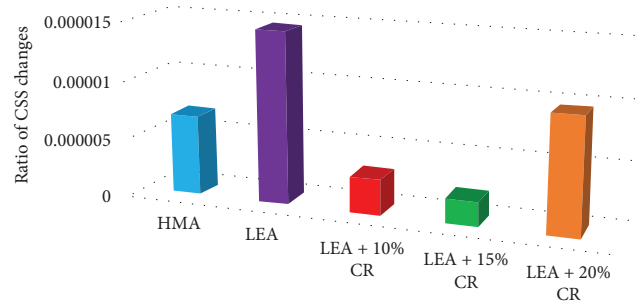


Figure 8: Ratio of creep strain slope changes.

reduced the sensitivity of these specimens to the stress level. In other words, the use of CR significantly decreased the dependence of permanent deformations on stress.

Also, in this research, the three-stage Zhou model was used as a suitable tool to better understand the behavior of

specimens against permanent deformation. One of the considerable advantages of using this model is its ability to derive mathematical relationships for different creep areas and to accurately determine the transition points between these areas. Tables 8 and 9 present the results obtained from the model proposed for the experimental specimens. The noteworthy point in these results is the formation of all three creep zones in all specimens. The reason for this is the appropriate selection of the maximum number of load cycles in the process of performing this test. Another point in relation to these results is the high correlation coefficients of the obtained equations and the results of the experiment, indicating that all the creep diagrams conform to the mentioned model.

Moreover, Figure 9 shows the number of load cycles at the end of the first zone ($N_{ps}$) for different specimens of asphalt mixtures at two stress levels of 207 and 310 kPa. As can be seen from the figure, as the stress level increases, the number of load cycles leading to the end of the first zone decreases. Since the first zone represents the elastic behavior and the second zone represents the viscoelastic behavior, increasing the stress level led to the acceleration of the change in the state of asphalt mixtures from the elastic state to the viscous state. In addition, according to Figure 10, the ratio of the values of this parameter at these stress levels shows that the lowest value is related to LEA specimens modified by 15% and 10% CR, and the highest value is associated with the base LEA. In other words, the use of CR delayed the change of the state of LEA specimens from elastic to viscous. Furthermore, Figure 9 shows that the LEA specimen containing 15% CR has the maximum length in the first zone at both stress levels. In other words, this specimen experiences the longest elastic state compared to other specimens, and the LEA specimen without the additive with the shortest length of the first zone is the most susceptible specimen to develop permanent deformation. Figure 11 also provides FN values for asphalt mixtures. FN is the number of cycles corresponding to the beginning of the third area, which has a good correlation with the rutting potential of asphalt mixtures. Since all deformations created in asphalt mixtures change to plastic by passing through the second zone, determining the beginning of the third zone can be considered a suitable criterion for evaluating the rutting resistance of asphalt mixtures [45]. It should be noted that Figure 11 is drawn based on the average FN values presented in Table 10. As mentioned earlier and can be seen in Table 10, for each level of stress, the dynamic shear test was repeated three times. Also, the standard deviation (SD) values for the mentioned repetitions are presented.

According to the results, the highest FN at both stress levels is related to the LEA specimen containing 15% CR and the lowest to the unmodified LEA. The values of this parameter for the LEA specimen modified by 15% CR at two stress levels of 207 and 310 kPa are 6.5 and 7 times higher than the LEA specimen without the additive, respectively. Also, the comparison of these results showed that the modification of LEA with the mentioned amount by CR caused a significant increase in the resistance of the specimen against rutting compared to HMA so that FN values for this specimen are 2.3 times higher than the number of cycles corresponding to the beginning of the third area in both stress levels than HMA specimen.

*3.2. Moisture Sensitivity.* Table 11 summarizes the results of the moisture sensitivity. Also, Figures 12 and 13 provide the ITS in dry and conditioned conditions for asphalt specimens, respectively. As can be seen, the ITS test was performed with three repetitions, and the average ITS obtained from each type of specimen was used in drawing Figures 12 and 13. It was revealed that the LEA specimen without the additive compared to the control specimen (HMA) experienced a significant reduction in ITS in both dry and conditioned states. Since part of the water vapor created in the LEA manufacturing process is trapped in the asphalt binder, this asphalt has pores for easier water penetration to the surface of aggregates [46]. Therefore, LEA experiences a more severe drop in the amount of ITS in the conditioned state than the HMA specimen. In this evaluation, ITS decrease rate in the LEA specimen without the additive compared to the HMA specimen in dry and conditioned states is 0.39 and 0.53, respectively. As mentioned in the previous sections, due to the poor performance of LEA mixtures, in this study, CR additive was used to coat them. The studies conducted on the performance of CR-modified mixtures against moisture failure show that these asphalt mixtures, despite their high resistance to rutting and fatigue, have low moisture resistance, and only a small content of CR in them can lead to a decrease in moisture sensitivity [47–50]. By adding CR to the asphalt binder, its viscosity increases. Since this increase causes a thicker coating of asphalt binder on aggregates, the slight use of this additive can lead to greater adhesion of binder and aggregates and finally increase the resistance of the mixture to moisture [51]. By increasing CR percentage, the viscosity of the binder improves significantly, and as a result, the workability of the mixture decreases during mixing. This has a negative effect on the coating of aggregate and leads to a reduction in adhesion and cohesion, as well as stiffness, and an increase in moisture sensitivity [47]. According to Figures 12 and 13, the use of CR increases ITS value for dry and conditioned states in LEA specimens. The amount of this increase continues up to 15% of CR. By increasing the percentage of CR from 15% to 20%, this parameter decreased, which was predictable due to what was explained.

Figure 14 shows the TSR of LEA and HMA specimens. According to the results, the highest value of this ratio was observed for the HMA specimen, and as expected, the lowest value of this parameter was recorded for the LEA specimen without the additive. High moisture sensitivity of the LEA specimen without the additive was due to the low viscosity of asphalt binder, inadequate coating of aggregates, and also easier infiltration of water due to large voids in the asphalt binder membrane around the aggregates. In this evaluation, the addition of CR to LEA specimens increased the moisture resistance of this type of asphalt mixture, and the highest moisture resistance among LEA specimens was recorded

Table 8: Three-stage model for the creep curves of the mixtures at 207 kPa stress level.

| Specimen | Primary stage | | | Secondary stage | | | Tertiary stage | |
|---|---|---|---|---|---|---|---|---|
| | Model | First point | $R^2$ | Model | End point | $R^2$ | Model | $R^2$ |
| HMA | $\varepsilon p = 0.02478\ N^{0.50064}$ | 1,744 | 0.99 | $\varepsilon p = 1.055 + 0.0003\ (N\text{-}1744)$ | 2,842 | 0.99 | $\varepsilon p = 1.434 + 1.97981\ (e^{0.00017(N\text{-}2842)} - 1)$ | 0.98 |
| LEA | $\varepsilon p = 0.03242\ N^{0.55263}$ | 706 | 0.99 | $\varepsilon p = 1.23 + 0.0011\ (N\text{-}706)$ | 1,006 | 0.99 | $\varepsilon p = 1.549 + 2.47383\ (e^{0.00041(N\text{-}1006)} - 1)$ | 0.98 |
| LEA + %10 CR | $\varepsilon p = 0.02069\ N^{0.47726}$ | 2,002 | 0.99 | $\varepsilon p = 0.787 + 0.0002\ (N\text{-}2002)$ | 3,802 | 0.99 | $\varepsilon p = 1.15 + 1.16863\ (e^{0.00017(N\text{-}3802)} - 1)$ | 0.99 |
| LEA + %15 CR | $\varepsilon p = 0.01312\ N^{0.48683}$ | 2,602 | 0.98 | $\varepsilon p = 0.606 + 0.0001\ (N\text{-}2602)$ | 6,610 | 0.99 | $\varepsilon p = 1.039 + 1.18221\ (e^{0.00011(N\text{-}6610)} - 1)$ | 0.99 |
| LEA + %20 CR | $\varepsilon p = 0.05489\ N^{0.44414}$ | 982 | 0.98 | $\varepsilon p = 1.136 + 0.0005\ (N\text{-}982)$ | 1,804 | 0.99 | $\varepsilon p = 1.519 + 1.46427\ (e^{0.0003(N\text{-}1804)} - 1)$ | 0.99 |

Table 9: Three-stage model for the creep curves of the mixtures at 310 kPa stress level.

| Specimen | Primary stage | | | Secondary stage | | | Tertiary stage | |
|---|---|---|---|---|---|---|---|---|
| | Model | First point | $R^2$ | Model | End point | $R^2$ | Model | $R^2$ |
| HMA | $\varepsilon p = 0.0297\ N^{0.5542}$ | 547 | 0.99 | $\varepsilon p = 0.981 + 0.001\ (N-547)$ | 1,309 | 0.99 | $\varepsilon p = 1.755 + 2.3842(e^{0.00046*(N-1309)} - 1)$ | 0.98 |
| LEA | $\varepsilon p = 0.0293\ N^{0.6337}$ | 145 | 0.99 | $\varepsilon p = 0.684 + 0.0026\ (N-145)$ | 427 | 0.99 | $\varepsilon p = 1.43 + 1.7223\ (e^{0.0015*(N-427)} - 1)$ | 0.99 |
| LEA +%10 CR | $\varepsilon p = 0.0205\ N^{0.5414}$ | 997 | 0.98 | $\varepsilon p = 0.867 + 0.0005\ (N-997)$ | 2,143 | 0.99 | $\varepsilon p = 1.456 + 1.0096\ (e^{0.00056\ (N-2143)} - 1)$ | 0.99 |
| LEA + %15 CR | $\varepsilon p = 0.0167\ N^{0.52591}$ | 1,282 | 0.99 | $\varepsilon p = 0.725 + 0.0003\ (N-1282)$ | 3,016 | 0.98 | $\varepsilon p = 1.246 + 1.1822\ (e^{0.00026\ (N-3016)} - 1)$ | 0.98 |
| LEA + %20 CR | $\varepsilon p = 0.0606\ N^{0.4953}$ | 355 | 0.99 | $\varepsilon p = 1.107 + 0.0015\ (N-355)$ | 754 | 0.99 | $\varepsilon p = 1.716 + 1.5257\ (e^{0.00106*(N-754)} - 1)$ | 0.99 |

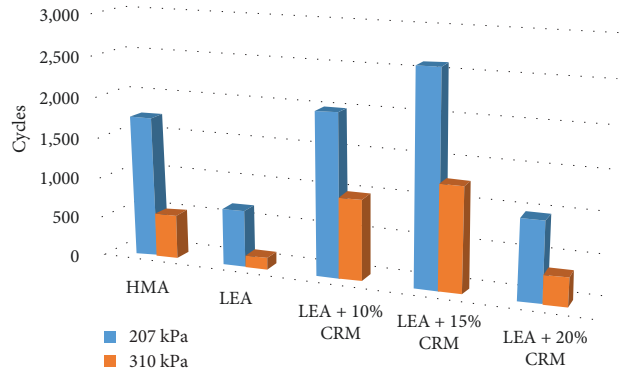


Figure 9: Number of load cycles at the end of the first stage ($N_{ps}$).

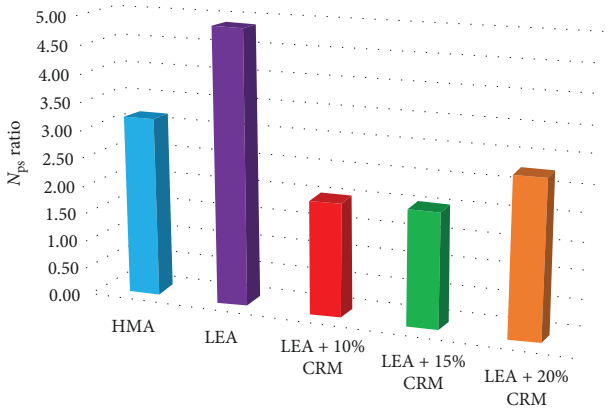


Figure 10: $N_{ps}$ ratio at two stress levels.

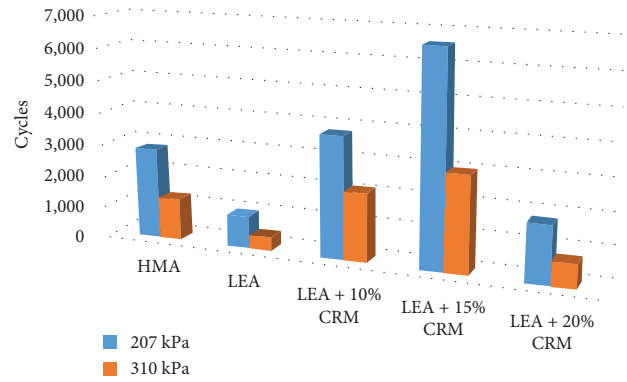


Figure 11: Number of load cycles at the end of the second stage ($N_{st}$).

Table 10: Dynamic creep test results at two stress levels.

| Specimen | Stress level | Test repetition 1 | 2 | 3 | Average FN | SD |
|---|---|---|---|---|---|---|
| HMA | 207 | 2,856 | 2,827 | 2,844 | 2,842 | 14.57 |
| | 310 | 1,311 | 1,288 | 1,327 | 1,309 | 19.60 |
| LEA | 207 | 1,006 | 989 | 1,023 | 1,006 | 17.00 |
| | 310 | 421 | 448 | 411 | 427 | 19.14 |
| LEA + %10 CR | 207 | 3,817 | 3,799 | 3,791 | 3,802 | 13.32 |
| | 310 | 2,135 | 2,149 | 2,144 | 2,143 | 7.09 |
| LEA + %15 CR | 207 | 6,612 | 6,619 | 6,600 | 6,610 | 9.61 |
| | 310 | 3,022 | 3,011 | 3,014 | 3,016 | 5.69 |
| LEA + %15 CR | 207 | 1,801 | 1,789 | 1,823 | 1,804 | 17.24 |
| | 310 | 747 | 763 | 751 | 754 | 8.33 |

for 10% CR-modified specimens. TSR value in this specimen increased by 22% compared to the LEA specimen without the additive.

A noteworthy point in the use of CR in LEA specimens is its negative effect on TSR at high percentages. As mentioned, the use of CR in asphalt mixtures indicates the effect of this additive on increasing moisture resistance at low percentages. This issue was expressed due to the achievement of good viscosity of asphalt binder in the use of CR in low percentages, which increases the asphalt binder film on the materials and their better coating. By increasing the percentage of CR from 10% to 20%, according to Table 5, the viscosity of asphalt binder increases dramatically; therefore, due to excessive stiffness, the asphalt binder is not able to properly coat the aggregates, and moisture has more opportunity to penetrate into its surface. As a result, TSR in these mixtures is reduced. Another point about the use of CR in LEA specimens is the inability of this additive to compensate for the drop in moisture resistance compared to the HMA specimen. As the results show, although the use of this additive reduced the moisture sensitivity of LEA specimens by 10%, the highest represented TSR for this specimen is still lower than TSR of HMA specimen. In addition, none of the LEA specimens is able to meet the minimum required TSR value defined in this test (80%). Therefore, the use of CR, despite its proven benefits in improving the performance characteristics of asphalt mixtures, can not improve the moisture sensitivity of LEA. Therefore, it seems necessary to use anti-striping agents to cover its low resistance to moisture.

*3.3. Fatigue Resistance Results.* One of the objectives of this study is to evaluate the fatigue resistance of LEA mixtures without the additive and modified by CR. For this purpose, to compare the fatigue life, different methods were applied based on the dissipated energy, and the results were compared with the fatigue life obtained from the traditional method or the recommended method based on AASHTO T321-07. According to the mentioned standard, the fatigue life of asphalt mixtures ($N_{f50}$) refers to the number of load cycles corresponding to a 50% reduction in initial stiffness. Figure 15 compares $N_{f50}$ diagram at the strain levels used. Each diagram was plotted based on the results of the fatigue test at two levels of strain, 400 and 700 $\mu$m. It should be noted that Figure 15 is drawn based on the average values of $N_{f50}$ presented in Table 12. The fatigue test was repeated three times for each level of strain. Also, SD values for the mentioned repetitions are evident.

The results clearly show that the highest fatigue life belongs to HMA. The longer fatigue life of HMA compared to LEA specimens is due to the greater adhesion of asphalt

Table 11: Indirect tensile strength test results in the dry and wet conditions.

| Specimen | Test repetition | $ITS_{dry}$ (kPa) | SD | Average $ITS_{dry}$ (kPa) | $ITS_{wet}$ (kPa) | SD | Average $ITS_{wet}$ (kPa) | TSR (%) |
|---|---|---|---|---|---|---|---|---|
| HMA | 1 | 956 | 8.89 | 946 | 782 | 3.61 | 785 | 83 |
| | 2 | 943 | | | 789 | | | |
| | 3 | 939 | | | 784 | | | |
| LEA | 1 | 573 | 3.21 | 575 | 361 | 6.11 | 368 | 64 |
| | 2 | 579 | | | 369 | | | |
| | 3 | 574 | | | 373 | | | |
| LEA + 10% CR | 1 | 721 | 5.69 | 726 | 559 | 7 | 567 | 78 |
| | 2 | 732 | | | 573 | | | |
| | 3 | 724 | | | 568 | | | |
| LEA + 15% CR | 1 | 839 | 10.07 | 848 | 593 | 7 | 594 | 70 |
| | 2 | 859 | | | 588 | | | |
| | 3 | 847 | | | 602 | | | |
| LEA + 20% CR | 1 | 799 | 4.04 | 795 | 475 | 6 | 477 | 60 |
| | 2 | 794 | | | 484 | | | |
| | 3 | 791 | | | 473 | | | |

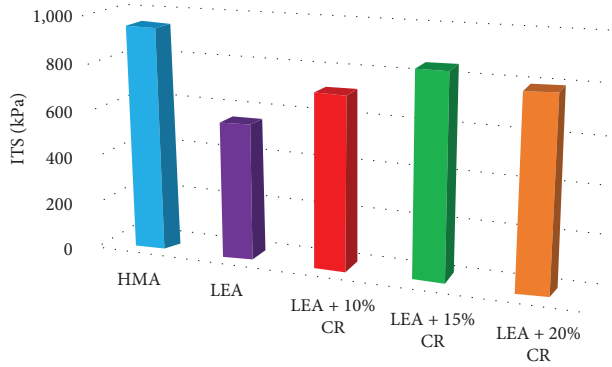


Figure 12: Indirect tensile strength values of mixtures in dry condition.

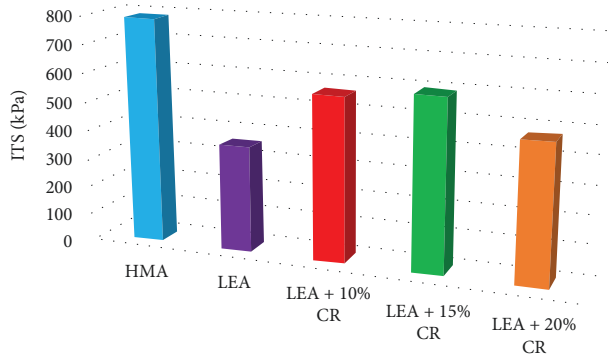


Figure 13: Indirect tensile strength values of mixtures in wet condition.

binder to aggregates and higher cohesion and coherence in the overall structure of the mixture. Also, LEA specimen without the additive provides the shortest fatigue life. The results confirm the findings of previous research on the fatigue resistance of LEA without the additive and its comparison with the HMA specimen [22–24].

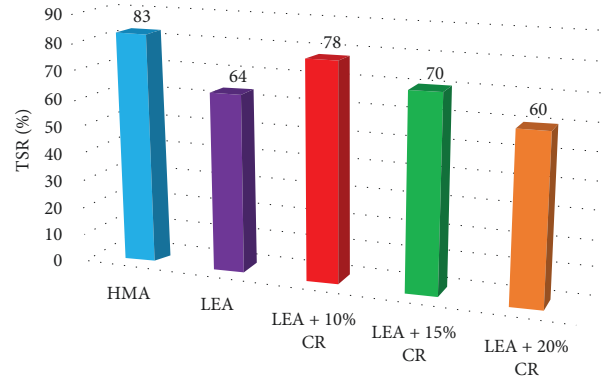


Figure 14: Tensile strength ratio values.

In general, the adhesion of asphalt binder and aggregates has a great role in the fatigue resistance of asphalt mixtures [52]. Therefore, the low fatigue resistance of the LEA specimen is considered to be due to the weaker adhesion of asphalt binder and aggregates because of the presence of water, and less adhesion and cohesion of the mixture. On the other hand, the use of CR in LEA specimens increased fatigue resistance, so that the LEA specimen containing 10% CR is in the same situation as the HMA specimen. By increasing CR percentage, the fatigue life of these specimens is reduced. This is due to the excessive absorption of the aromatic part in the asphalt binder and the brittleness of the mixture. Therefore, the modified specimen containing 10% CR showed the best performance among other LEA specimens. Another parameter that can be extracted to evaluate the fatigue resistance is the initial stiffness of asphalt mixtures. According to the mentioned standard, the initial stiffness is the stiffness corresponding to the 50th cycle. Figure 16 provides this criterion for asphalt mixtures in strains of 400 and 700 $\mu\varepsilon$. As can be seen, the LEA specimen containing 10% CR at a strain of 400 is in the same situation as the HMA specimen. By increasing the strain level to

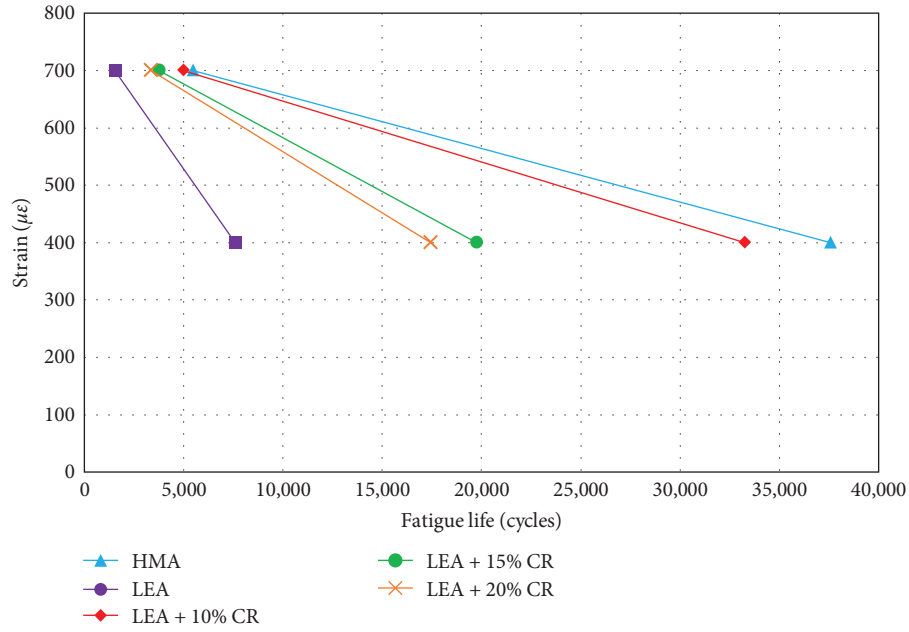


Figure 15: Comparison of fatigue lives for asphalt mixtures based on the classical procedure.

Table 12: Fatigue test results at two stress levels.

| Specimen | Stress level | Test repetition | | | Average $N_{f50}$ | SD |
|---|---|---|---|---|---|---|
| | | 1 | 2 | 3 | | |
| HMA | 400 | 37,556 | 37,571 | 37,548 | 37,558 | 11.7 |
| | 700 | 5,465 | 5,460 | 5,453 | 5,459 | 6.0 |
| LEA | 400 | 7,571 | 7,609 | 7,593 | 7,591 | 19.1 |
| | 700 | 1,537 | 1,532 | 1,526 | 1,532 | 5.5 |
| LEA + %10 CR | 400 | 17,429 | 17,454 | 17,419 | 17,434 | 18.0 |
| | 700 | 3,364 | 3,353 | 3,347 | 3,355 | 8.6 |
| LEA + %15 CR | 400 | 19,731 | 19,755 | 19,746 | 19,744 | 12.1 |
| | 700 | 3,749 | 3,745 | 3,763 | 3,752 | 9.5 |
| LEA + %15 CR | 400 | 33,248 | 33,241 | 33,237 | 33,242 | 5.6 |
| | 700 | 4,965 | 4,982 | 4,967 | 4,971 | 9.3 |

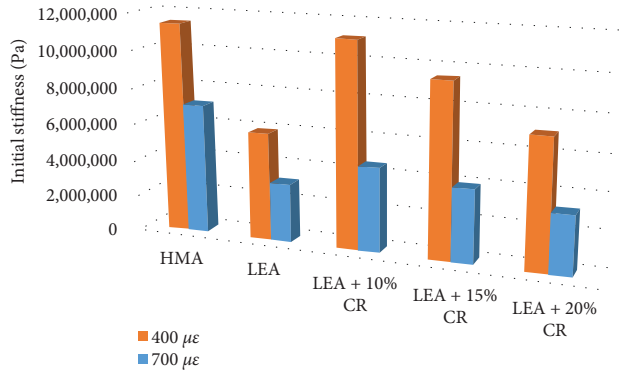


Figure 16: Comparison of initial stiffness for asphalt mixtures.

700 $\mu\varepsilon$, although this specimen has the highest fatigue resistance compared to other LEA specimens, its initial stiffness was reduced by about 35% compared to the HMA specimen.

Figure 17 shows the fatigue life of asphalt mixtures based on $N_{ER}$, $N_{S\times n}$, $N_{f50}$ criteria at 400 $\mu\varepsilon$. At a strain of 400 $\mu\varepsilon$, as can be seen in the results, in all the methods used, the maximum fatigue life belongs to the HMA specimen, followed by a specimen containing 10% CR with a slight difference. The fatigue life obtained by $N_{ER}$, $N_{S\times n}$, $N_{f50}$ methods for LEA specimens containing 10% CR is about 0.89, 0.81, and 0.97 times that of HMA specimens, respectively. Also, the unmodified LEA specimen has the shortest fatigue life, and the fatigue life based on the mentioned parameters for this specimen is 0.2, 0.21, and 0.12 times compared to the HMA specimen, respectively. At this strain level, LEA specimens containing 15% and 20% CR are in the same situation. Moreover, by comparing the fatigue life obtained from these methods, it is clear that in all experimental specimens, the fatigue life obtained from the $N_{S\times n}$ method has the highest value compared to other methods. At a strain of 400 $\mu\varepsilon$, the

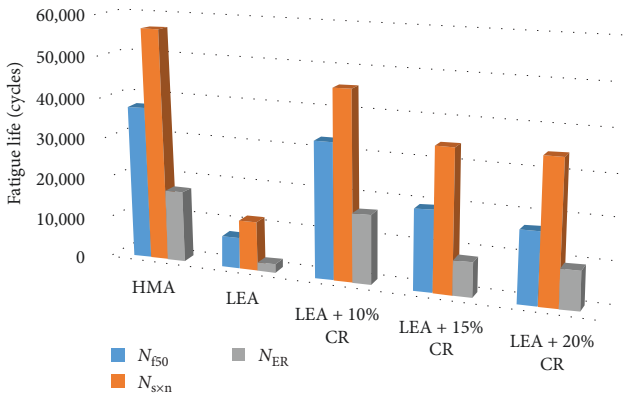


FIGURE 17: Comparison between the fatigue lives obtained from different definitions at the strain of 400 $\mu\varepsilon$.

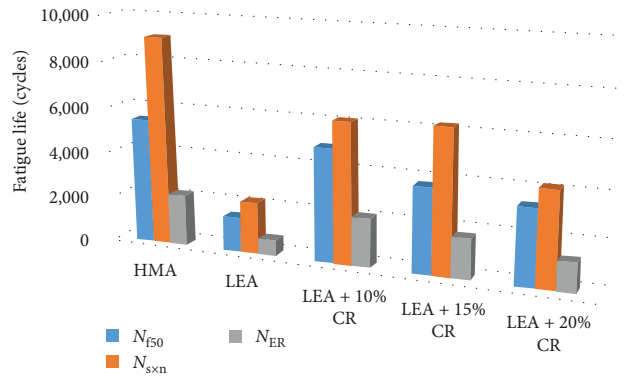


FIGURE 18: Comparison between the fatigue lives obtained from different definitions at the strain of 700 $\mu\varepsilon$.

fatigue life calculated by this method in the HMA specimen is 1.51 and 3.24 times longer than $N_{f50}$ and $N_{ER}$ methods, respectively. Also, according to Figure 18 and comparing the fatigue lives obtained at a strain of 700 $\mu\varepsilon$, it can be concluded that the obtained fatigue lives follow a similar process to the achieved results at a strain of 400 $\mu\varepsilon$. The difference is that among LEA specimens, the fatigue life calculated by the $N_{S\times n}$ method has the highest value for the modified specimen containing 15% CR.

As described in Section 2.4.3, IDE is not very reliable as a criterion for comparing the fatigue behavior of asphalt mixtures. This criterion is applicable when asphalt mixtures are similar in terms of the type of material, asphalt binder, and manufacturing conditions. On the other hand, some researchers believe that CDE is not a suitable parameter to describe the fatigue resistance of asphalt mixtures. This parameter can not distinguish the dissipated energy due to the failure phenomenon from the energy released due to the viscoelastic behavior of the mixture. At first, it was assumed that the total dissipated energy would lead to the failure of asphalt mixture in each load cycle. However, later research showed that part of dissipated energy occurs due to plastic deformation and heat generation [53–55]. Therefore, the researchers presented RDEC to evaluate the fatigue properties of asphalt mixtures according to Equation (12).

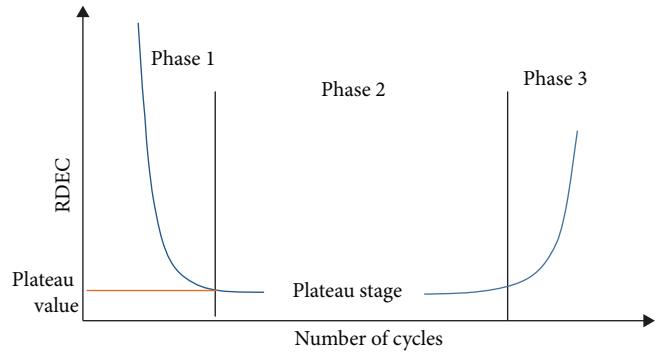


FIGURE 19: Schematic diagram of RDEC versus load cycles [56].

Figure 19 shows the changes in this parameter against the number of load cycles. As can be seen, this curve consists of three parts. In the initial part, the value of this parameter decreases sharply with the increase of the load cycle. In the second region, the curve experiences a stable state called the plateau stage. In the third region, RDEC experiences a sudden increase in the actual failure of the specimen. A significant part of this curve is the second zone, where a constant percentage of the applied energy leads to failure in the asphalt mixture. In this area, the RDEC value is called the plateau value (PV), where the initial stiffness reaches 50% of its value. PV provides a constant rate of input energy that is converted to failure. This parameter has a strong relationship with the fatigue life of asphalt mixture due to its nondependence on the type of mixture and test conditions. Hence, it provides a complete definition of the fatigue characteristics of asphalt mixtures [40, 53, 56]. According to the mentioned definition, the amount of PV is determined by Equation (12), where PV is the plateau value, $N_{f50}$ is the fatigue life of asphalt mixture corresponding to a 50% reduction in initial stiffness, $K$ represents the slope of dissipated energy curve versus the load cycle.

$$\mathrm{PV} = \frac{1 - \left(1 + \frac{100}{N_{f50}}\right)^{K}}{100}. \tag{12}$$

Figure 20 shows PV values of LEA and HMA specimens. In evaluating the fatigue resistance of asphalt mixtures, it should be noted that mixtures with higher resistance have lower PV values [57]. Accordingly, at both strain levels, among asphalt specimens, the HMA specimen had the lowest PV and the highest fatigue resistance. Also, the LEA specimen without the additive had the highest PV, so this specimen showed the weakest fatigue resistance. By modifying the asphalt binder by CR, the LEA specimen containing 10% additive represented the best performance among other LEA specimens, so that PV value in this specimen had the lowest difference compared to the HMA specimen. As CR percentage increases, the amount of PV in LEA specimens experienced an almost identical process in increasing this parameter. In other words, increasing the percentage of CR reduced the fatigue resistance of this type of asphalt.

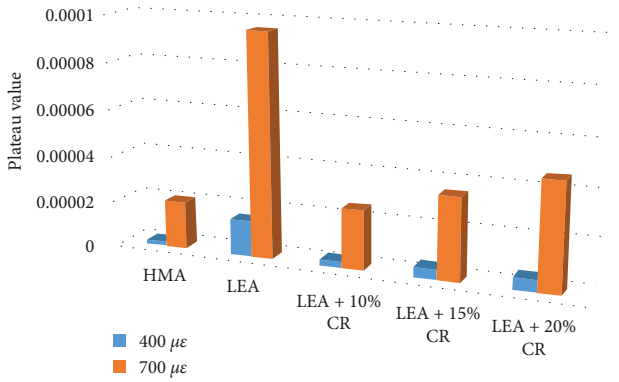


FIGURE 20: Comparison between PV parameters for asphalt mixtures.

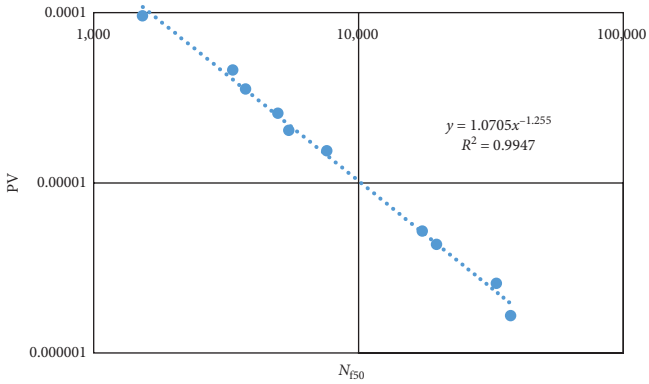


FIGURE 21: Relationship between PV and $N_{f50}$ for all studied mixtures at two strain levels.

Moreover, by comparing PV values at 400 and 700 $\mu\varepsilon$, it can be concluded that increasing the strain level reduced the difference in the values of this parameter in LEA specimens compared to HMA. In other words, LEA specimens had more resistance to fatigue at higher strains. For example, PV ratio for a specimen containing 10% CR compared to HMA changed from 1.54 to 1.26 with increasing strain from 400 to 700 $\mu\varepsilon$.

In addition, Figure 21 shows the relationship between PV and $N_{f50}$ on a logarithmic–logarithmic scale. Unlike the traditional method, where each mixture provides a separate relationship, this method can provide a unique relationship for asphalt mixtures. In other words, in the assessment of fatigue resistance by the RDEC method, the type of materials, manufacturing method, and mixing and compaction temperatures do not affect the results of fatigue resistance. Equation (13) shows the mathematical equation of the relationship between PV and $N_{f50}$ for the experimental specimens, in which, according to the $R^2$ value, a strong correlation can be found in this relationship.

$$\mathrm{PV} = 1.0705\left(N_{f50}\right)^{-1.255},\ R^2 = 0.9947. \tag{13}$$

## 4. Conclusion

Given the concerns of human society about the increase in environmental pollution and excessive energy consumption, in this research, the performance characteristics of LEA as an alternative to HMA were evaluated. In order to cover the performance weaknesses of LEA, the modification of LEA by CR additive at 10%, 15%, and 20% was the main goal of this research. The dynamic creep, modified Lottman, and four-point bending beam tests were used to evaluate the rutting resistance, moisture sensitivity, and fatigue resistance of LEA and HMA mixtures. Based on the findings of this study, significant results were extracted, which are described below:

(1) Accumulated strain diagrams in the dynamic creep test showed that LEA specimens containing 15% and 10% CR had better performance against rutting than HMA, respectively. Also, LEA without the additive was represented as the weakest specimen due to its excessive softness, and the LEA specimen modified by 20% CR had lower stiffness due to the weakness of asphalt binder in proper coverage of aggregates, low integrity and cohesion of the mixture; as a result, it represented a lower resistance to rutting than HMA.

(2) The number of load cycles at 1% strain showed that the highest load cycle belonged to LEA specimens modified by 15% and 10% CR, as well as HMA specimens, respectively. Moreover, the lowest load cycle was observed for LEA specimens containing 20% CR and LEA specimens without the additive. Also, the evaluation of the CSS change rate confirmed that LEA modification with the mentioned values significantly reduced the sensitivity of these specimens to the increase in stress levels.

(3) Modeling of creep diagrams based on Zhou's 3-stage model showed that the mentioned model has a high ability to interpret these curves. Also, extracting Nst and FN in this model presented the best performance for LEA containing 15% and 10% CR, respectively.

(4) In the ITS test, the highest moisture resistance was assigned to the HMA specimen, and the lowest moisture sensitivity among LEA specimens was recorded for modified LEA containing 10% CR. Moreover, it was found that despite its effect on increasing resistance, CR can not compensate for the reduction of TSR in LEA. Therefore, it seems necessary to use anti-stripping agents in the process of making this asphalt.

(5) In the evaluation of fatigue resistance by the classical method, it was determined that the LEA specimen containing 10% CR had $N_{f50}$ and initial stiffness almost similar to HMA. Also, other LEA specimens showed lower fatigue resistance. The reason for this was the poor adhesion of binder and aggregates and the low integrity and cohesion of the mixture.

(6) By evaluating the fatigue resistance by the dissipated energy method and determining the fatigue life by $N_{ER}$ and $N_{S\times n}$ criteria, it was found that the modified LEA specimen by 10% CR had almost the same fatigue life compared to HMA specimen. Furthermore, while modified LEA specimens containing 15% and 20% CR were in a similar situation, the lowest fatigue life was assigned to LEA specimens without the additive.

(7) The fatigue resistance evaluation by the RDEC method indicated the lowest PV value for HMA and LEA modified by 10% CR, respectively. Although unmodified LEA had the highest PV by a significant difference, modified LEA specimens containing 15% and 20% CR had an almost similar upward trend in increasing this parameter with increasing CR content.

(8) For future studies, statistical analysis can be incorporated into the proposed approaches [58–61]. Moreover, various modeling methods are recommended for further investigation [62–65]. Optimization algorithms are also recommended to obtain the optimal additive content [66–68]. Various validation methods are recommended in this regard [69, 70]. Fourier transform infrared spectroscopy and X-ray fluorescence spectroscopy can be utilized to identify and quantify the chemical composition of materials [71–73]. Pavement texture and surface play a crucial role in determining the distribution of stresses and strains experienced by the pavement structure, which can be examined in the future [74–78]. The material size can also affect the resistance, which can be investigated further [79, 80]. Furthermore, the effect of various antistripping agents, polymers, and nanomaterials is recommended to be investigated on the performance of LEA mixtures [81–86]. Moreover, other performances of CR-modified LEA mixtures can be evaluated in the future [87, 88].

## Data Availability

The data used to support the findings of this study are available from the corresponding author upon request.

## Disclosure

In this study, Iranian governmental organizations have not been partners and sponsors, and this study is purely studious.

## Conflicts of Interest

The authors declare that they have no conflicts of interest.

## References

[1] M. R. Gruber and B. Hofko, "Life cycle assessment of greenhouse gas emissions from recycled asphalt pavement production," *Sustainability*, vol. 15, no. 5, Article ID 4629, 2023.

[2] B. Panda, F. M. Rad, and M. S. Rajabi, "Wireless charging of electric vehicles through pavements: system, design, and technology," in *Handbook of Smart Energy Systems*, M. Fathi, E. Zio, and P. M. Pardalos, Eds., pp. 1–26, Springer, Cham, 2023.

[3] M. R. Yazdi-Samadi, "Exploring the investment cost of construction of renewable power plant considering the effect of climate impact," *Energy*, vol. 2022, Article ID 2965, 2004.

[4] A. Kazemtarghi, S. Dey, A. Mallik, and N. G. Johnson, "Asymmetric half-frequency modulation in DAB to optimize the conduction and switching losses in EV charging applications," *IEEE Transactions on Transportation Electrification*, pp. 1–1, 2023.

[5] A. Razmjoo, A. Ghazanfari, M. Jahangiri et al., "A comprehensive study on the expansion of electric vehicles in Europe," *Applied Sciences*, vol. 12, no. 22, Article ID 11656, 2022.

[6] M. Sadeghi, M. Nikfar, and F. M. Rad, "Optimizing warehouse operations for environmental sustainability: a simulation study for reducing carbon emissions and maximizing space utilization," *Journal of Future Sustainability*, vol. 4, pp. 35–44, 2024.

[7] Z. Cao, M. Chen, J. Yu, and X. Han, "Preparation and characterization of active rejuvenated SBS modified bitumen for the sustainable development of high-grade asphalt pavement," *Journal of Cleaner Production*, vol. 273, Article ID 123012, 2020.

[8] M. Kazemidemneh and M. Mahdavinejad, "Use of space syntax technique to improve the quality of lighting and modify energy consumption patterns in urban spaces," *European Journal of Sustainable Development*, vol. 7, no. 2, pp. 29–40, 2018.

[9] M. Zarei, A. A. Kordani, A. Naseri, M. W. Khordehbinan, M. khajehzadeh, and M. Zahedi, "Evaluation of fracture behaviour of modified warm mix asphalt containing vertical and angular cracks under freeze–thaw damage," *International Journal of Pavement Engineering*, pp. 1–17, 2022.

[10] S. A. Ziaee, F. Moghadas Nejad, M. Dareyni, and M. Fakhri, "Evaluation of rheological and mechanical properties of hot and warm mix asphalt mixtures containing Electric Arc Furnace Slag using gyratory compactor," *Construction and Building Materials*, vol. 378, Article ID 131042, 2023.

[11] F. Moghadas Nejad, A. Azarhoosh, G. H. Hamedi, and H. Roshani, "Rutting performance prediction of warm mix asphalt containing reclaimed asphalt pavements," *Road Materials and Pavement Design*, vol. 15, no. 1, pp. 207–219, 2014.

[12] M. A. Kadhim, S. Al-Busaltan, A. Dulaimi et al., "Developing a sustainable, post treated, half warm mix asphalt for structural surface layer," *Construction and Building Materials*, vol. 342, Article ID 127926, 2022.

[13] A. Vaitkus, D. Čygas, A. Laurinavičius, V. Vorobjovas, and Z. Perveneckas, "Influence of warm mix asphalt technology on asphalt physical and mechanical properties," *Construction and Building Materials*, vol. 112, pp. 800–806, 2016.

[14] B. Kheradmand, R. Muniandy, L. T. Hua, R. B. Yunus, and A. Solouki, "An overview of the emerging warm mix asphalt technology," *International Journal of Pavement Engineering*, vol. 15, no. 1, pp. 79–94, 2014.

[15] F. Olard and A. Romier, "Low emission and low energy asphalts for sustainable road construction the European experience of LEA process," Retrieved from LEA-UK, 2011.

[16] G. A. Harder, Y. LeGoff, A. Loustau, Y. Martineau, B. Heritier, and A. Romier, *Energy and Environmental Gains of Warm and Half-Warm Asphalt Mix: Quantitative Approach*, Transportation Research Board, Washington, DC United States, 5th edition, 2008.

[17] A. Romier, M. Audeon, J. David, Y. Martineau, and Fçois Olard, "Low-energy asphalt with performance of hot-mix asphalt," *Transportation Research Record: Journal of the Transportation Research Board*, vol. 1962, no. 1, pp. 101–112, 2006.

[18] V. Gaudefroy, *Laboratory Environmental Assessment of Half-Warm Mix Asphalts by Means of the Factorial Experiment Design Approach*, TRB Annual Meeting, 2009.

[19] A. Carter, O. Mainardis, and D. Perraton, *Design of Half-warm Asphalt Mixes With Additives*, Transportation Research Board, Washington, DC United States, 5th edition, 2010.

[20] R. F. Bonaquist, *Mix Design Practices for Warm Mix Asphalt*, Transportation Research Board, 2011.

[21] G. Harder, *LEA Half-Warm Mix Paving Report, 2007 Projects for NYSDOT*, McConnaughay Technologies, Cortland, NY, 2008.

[22] F. Olard and V. Gaudefroy, "Laboratory assessment of mechanical performance and fume emissions of LEA® HWMA (90 C) vs. traditional HMA (160 C)," in *2nd International Warm-Mix Conference*, pp. 1–16, ill, France, October 2012.

[23] S. C. Some, V. Gaudefroy, and D. Delaunay, "Warm mix asphalt: mechanical performance assessment and coating quality evaluation," in *2nd International Symposium on Asphalt Pavement and Environment*, pp. 1–12, ill, Paris, France, October 2012.

[24] H. Zelelew, C. Paugh, M. Corrigan, S. Belagutti, and J. Ramakrishnareddy, "Laboratory evaluation of the mechanical properties of plant-produced warm-mix asphalt mixtures," *Road Materials and Pavement Design*, vol. 14, no. 1, pp. 49–70, 2013.

[25] M. Samadi and N. Jahan, "Determining the effective level of outrigger in preventing collapse of tall buildings by IDA with an alternative damage measure," *Engineering Structures*, vol. 191, pp. 104–116, 2019.

[26] M. Samadi and N. Jahan, "Comparative study on the effect of outrigger on seismic response of tall buildings with braced and RC wall core. I: Optimum level and examining modal response spectrum analysis reliability," *The Structural Design of Tall and Special Buildings*, vol. 30, no. 8, Article ID e1848, 2021.

[27] R. Vahid, F. Farnood Ahmadi, and N. Mohammadi, "Earthquake damage modeling using cellular automata and fuzzy rule-based models," *Arabian Journal of Geosciences*, vol. 14, Article ID 1274, 2021.

[28] S. Razi, X. Wang, N. Mehreganian, M. Tootkaboni, and A. Louhghalam, "Application of mean-force potential lattice element method to modeling complex structures," *International Journal of Mechanical Sciences*, vol. 260, Article ID 108653, 2023.

[29] S. Bressi, N. Fiorentini, J. Huang, and M. Losa, "Crumb rubber modifier in road asphalt pavements: state of the art and statistics," *Coatings*, vol. 9, no. 6, Article ID 384, 2019.

[30] J. C. Munera and E. A. Ossa, "Polymer modified bitumen: optimization and selection," *Materials & Design (1980-2015)*, vol. 62, pp. 91–97, 2014.

[31] V. Najafi Moghaddam Gilani, S. M. Hosseinian, and M. Nikookar, "Presentation of a new deicer with the least moisture and fatigue failures in asphalt mixtures," *Arabian Journal for Science and Engineering*, vol. 46, pp. 10457–10471, 2021.

[32] M. Nikookar, M. B. Movahhed, J. Ayoubinejad, V. N. M. Gilani, and S. M. Hosseinian, "Improving the moisture sensitivity of asphalt mixtures by simultaneous modification of asphalt binder and aggregates with carbon nanofiber and carbon nanotube," *Advances in Civil Engineering*, vol. 2021, Article ID 6682856, 11 pages, 2021.

[33] V. N. M. Gilani, S. M. Hosseinian, H. Behbahani, and G. H. Hamedi, "Prediction and pareto-based multi-objective optimization of moisture and fatigue damages of asphalt mixtures modified with nano hydrated lime," *Construction and Building Materials*, vol. 261, Article ID 120509, 2020.

[34] G. H. Hamedi, M. R. Esmaeeli, V. N. M Gilani, and S. M. Hosseinian, "The effect of aggregate-forming minerals on thermodynamic parameters using surface free energy concept and its relationship with the moisture susceptibility of asphalt mixtures," *Advances in Civil Engineering*, vol. 2021, Article ID 8818681, 15 pages, 2021.

[35] T. B. Moghaddam, M. Soltani, and M. R. Karim, "Evaluation of permanent deformation characteristics of unmodified and polyethylene terephthalate modified asphalt mixtures using dynamic creep test," *Materials & Design*, vol. 53, pp. 317–324, 2014.

[36] H. Taherkhani and S. Afroozi, "Investigating the creep properties of asphaltic concrete containing nano-silica," *Sādhanā*, vol. 43, Article ID 24, 2018.

[37] N. B. Jomoor, M. Fakhri, and M. R. Keymanesh, "Determining the optimum amount of recycled asphalt pavement (RAP) in warm stone matrix asphalt using dynamic creep test," *Construction and Building Materials*, vol. 228, Article ID 116736, 2019.

[38] H. Y. Katman, M. R. Ibrahim, M. R. Karim, N. Salim Mashaan, and S. Koting, "Evaluation of permanent deformation of unmodified and rubber-reinforced SMA asphalt mixtures using dynamic creep test," *Advances in Materials Science and Engineering*, vol. 2015, Article ID 247149, 11 pages, 2015.

[39] H. Omrani, A. Tanakizadeh, A. R. Ghanizadeh, and M. Fakhri, "Investigating different approaches for evaluation of fatigue performance of warm mix asphalt mixtures," *Materials and Structures*, vol. 50, Article ID 149, 2017.

[40] A. Akbari and A. Modarres, "Fatigue response of HMA containing modified bitumen with nano-clay and nano-alumina and its relationship with surface free energy parameters," *Road Materials and Pavement Design*, vol. 21, no. 6, pp. 1490–1513, 2020.

[41] A. C. Pronk and P. C. Hopman, "Energy dissipation: the leading factor of fatigue. the United States strategic highway research program. sharing the benefits," in *Conference Organized by the Institution of Civil Engineers in Cooperation With US Strategic Highway Research Program, 29TH-31ST*, Elsevier Applied Science Publishers Limited, Tara Hotel, Kensington, London, October 1990.

[42] B. K. Bairgi, M. A. Hasan, and R. A. Tarefder, "Effects of asphalt foaming on damage characteristics of foamed warm mix asphalt," *Transportation Research Record: Journal of the Transportation Research Board*, vol. 2675, no. 8, pp. 318–331, 2021.

[43] M. Ameri, M. Seif, M. Abbasi, M. Molayem, and A. KhavandiKhiavi, "Fatigue performance evaluation of modified asphalt binder using of dissipated energy approach," *Construction and Building Materials*, vol. 136, pp. 184–191, 2017.

[44] M. E. Abdullah, K. A. Zamhari, M. R. Hainin, E. A. Oluwasola, N. I. Md. Yusoff, and N. A. Hassan, "High temperature characteristics of warm mix asphalt mixtures with nanoclay and chemical warm mix asphalt modified binders," *Journal of Cleaner Production*, vol. 122, pp. 326–334, 2016.

[45] N. Kamboozia, H. Ziari, and H. Behbahani, "Artificial neural networks approach to predicting rut depth of asphalt concrete by using of visco-elastic parameters," *Construction and Building Materials*, vol. 158, pp. 873–882, 2018.

[46] G. Shiva Kumar and S. Suresha, "State of the art review on mix design and mechanical properties of warm mix asphalt," *Road Materials and Pavement Design*, vol. 20, no. 7, pp. 1501–1524, 2019.

[47] H. H. Joni and A. H. Abed, "Evaluation the moisture sensitivity of asphalt mixtures modified with waste tire rubber," in *2nd International Conference of Al-Esraa University College for Engineering Sciences (ICAUC_ES 2021)*, vol. 961 of *IOP Conference Series: Earth and Environmental Science*, Article ID 012029, IOP Publishing Ltd., 2022.

[48] A. Ameli, N. Norouzi, E. H. Khabbaz, and R. Babagoli, "Influence of anti stripping agents on performance of binders and asphalt mixtures containing crumb rubber and styrene-butadiene-rubber," *Construction and Building Materials*, vol. 261, Article ID 119880, 2020.

[49] A. Cetin, "Effects of crumb rubber size and concentration on performance of porous asphalt mixtures," *International Journal of Polymer Science*, vol. 2013, Article ID 789612, 10 pages, 2013.

[50] H. Ziari, H. Divandari, S. M. Seyed Ali Akbar, and S. M. Hosseinian, "Investigation of the effect of crumb rubber powder and warm additives on moisture resistance of SMA mixtures," *Advances in Civil Engineering*, vol. 2021, Article ID 6653594, 12 pages, 2021.

[51] X. Wang, Z. Fan, L. Li, H. Wang, and M. Huang, "Durability evaluation study for crumb rubber-asphalt pavement," *Applied Sciences*, vol. 9, no. 16, Article ID 3434, 2019.

[52] P. V. Peltonen, "Road aggregate choice based on silicate quality and bitumen adhesion," *Journal of transportation engineering*, vol. 118, no. 1, 1992.

[53] S. Shen, *Dissipated Energy Concepts for HMA Performance: Fatigue and Healing*, ILLINOIS LIBRARY, 2006.

[54] C. Maggiore, G. Airey, and P. Marsac, "A dissipated energy comparison to evaluate fatigue resistance using 2-point bending," *Journal of Traffic and Transportation Engineering (English Edition)*, vol. 1, no. 1, pp. 49–54, 2014.

[55] A. Akbari and A. Modarres, "Evaluating the effect of nano-clay and nano-alumina on the fatigue response of bitumen using strain and time sweep tests," *International Journal of Fatigue*, vol. 114, pp. 311–322, 2018.

[56] M. Ameri, S. Yeganeh, and P. E. Valipour, "Experimental evaluation of fatigue resistance of asphalt mixtures containing waste elastomeric polymers," *Construction and Building Materials*, vol. 198, pp. 638–649, 2019.

[57] E. Santagata, O. Baglieri, L. Tsantilis, and G. Chiappinelli, "Fatigue properties of bituminous binders reinforced with carbon nanotubes," *International Journal of Pavement Engineering*, vol. 16, no. 1, pp. 80–90, 2015.

[58] F. Faghihinejad and S. Monajem, "Pathology of the disabled people access to public transport and prioritizing practical solution," *Tobacco Regulatory Science*, vol. 7, no. 6-1, 2021.

[59] G. Shen, C. Han, B. Chen, L. Dong, and P. Cao, "Fault analysis of machine tools based on grey relational analysis and main factor analysis," in *3rd Annual International Conference on Information System and Artificial Intelligence (ISAI2018)*, vol. 1069 of *Journal of Physics: Conference Series*, Article ID 012112, IOP Publishing Ltd., June 2018.

[60] F. Faghihinejad, M. Mohammadi Fard, A. Roshanghalb, and P. Beigi, "A framework to assess the correlation between transportation infrastructure access and economics: evidence from Iran," *Mathematical Problems in Engineering*, vol. 2022, Article ID 8781686, 15 pages, 2022.

[61] Z. Li, C. Han, and D. W. Coit, "System reliability models with dependent degradation processes," in *Advances in Reliability and Maintainability Methods and Engineering Applications*, Y. Liu, D. Wang, J. Mi, and H. Li, Eds., Springer Series in Reliability Engineering, pp. 475–497, Springer, 2023.

[62] M. A. Majdzadeh, A. Ghazanfari, and M. M. Ara, "Determinants of private investment in Iran based on Bayesian Model Averaging," *International journal of academic research in business and social sciences*, vol. 4, no. 7, pp. 229–240, 2014.

[63] H. Seraji, R. Tavakkoli-Moghaddam, and R. Soltani, "A two-stage mathematical model for evacuation planning and relief logistics in a response phase," *Journal of Industrial and Systems Engineering*, vol. 12, no. 1, pp. 129–146, 2019.

[64] C. Han and X. Fu, "Challenge and opportunity: deep learning-based stock price prediction by using bi-directional LSTM model," *Frontiers in Business, Economics and Management*, vol. 8, no. 2, pp. 51–54, 2023.

[65] Y. Xiao, X. Zuo, J. Huang, A. Konak, and Y. Xu, "The continuous pollution routing problem," *Applied Mathematics and Computation*, vol. 387, Article ID 125072, 2020.

[66] G. Shen, W. Zeng, Y. Zhang, C. Han, and P. Liu, "Determination of the average maintenance time of CNC machine tools based on type II failure correlation," *Eksploatacja i Niezawodnosc - Maintenance and Reliability*, vol. 19, no. 4, pp. 604–614, 2017.

[67] H. Seraji, R. Tavakkoli-Moghaddam, S. Asian, and H. Kaur, "An integrative location-allocation model for humanitarian logistics with distributive injustice and dissatisfaction under uncertainty," *Annals of Operations Research*, vol. 319, pp. 211–257, 2022.

[68] A. Kazemtarghi, S. Dey, and A. Mallik, "Optimal utilization of bidirectional EVs for grid frequency support in power systems," *IEEE Transactions on Power Delivery*, vol. 38, no. 2, pp. 998–1010, 2022.

[69] S. Haghir, R. Haghnazar, S. Saghafi Moghaddam, D. Keramat, M. R. Matini, and K. Taghizade, "BIM based decision-support tool for automating design to fabrication process of freeform lattice space structure," *International Journal of Space Structures*, vol. 36, no. 3, pp. 164–179, 2021.

[70] R. M. Rastegar, S. Saghafi Moghaddam, R. Haghnazar, and C. Zimring, "From evidence to assessment: developing a scenario-based computational design algorithm to support informed decision-making in primary care clinic design workflow," *International Journal of Architectural Computing*, vol. 20, no. 3, pp. 567–586, 2022.

[71] Z. Wang, Q. Wang, C. Jia, and J. Bai, "Thermal evolution of chemical structure and mechanism of oil sands bitumen," *Energy*, vol. 244, Part B, Article ID 123190, 2022.

[72] S. Zhou, C. Lu, X. Zhu, and F. Li, "Preparation and characterization of high-strength geopolymer based on BH-1 lunar soil simulant with low alkali content," *Engineering*, vol. 7, no. 11, pp. 1631–1645, 2021.

[73] M. Jin, Y. Ma, W. Li et al., "Multi-scale investigation on composition-structure of C-(A)-S-H with different Al/Si ratios under attack of decalcification action," *Cement and Concrete Research*, vol. 172, Article ID 107251, 2023.

[74] H. Wang, X. Zhang, and S. Jiang, "A laboratory and field universal estimation method for tire–pavement interaction noise (TPIN) based on 3D image technology," *Sustainability*, vol. 14, no. 19, Article ID 12066, 2022.

[75] H. Wang, X. Zhang, and M. Wang, "Rapid texture depth detection method considering pavement deformation calibration," *Measurement*, vol. 217, Article ID 113024, 2023.
[76] Z. Luo, H. Wang, and S. Li, "Prediction of international roughness index based on stacking fusion model," *Sustainability*, vol. 14, no. 12, Article ID 6949, 2022.
[77] Z. Lin, H. Wang, and S. Li, "Pavement anomaly detection based on transformer and self-supervised learning," *Automation in Construction*, vol. 143, Article ID 104544, 2022.
[78] C. Liu, J. Cui, Z. Zhang, H. Liu, X. Huang, and C. Zhang, "The role of TBM asymmetric tail-grouting on surface settlement in coarse-grained soils of urban area: field tests and FEA modelling," *Tunnelling and Underground Space Technology*, vol. 111, Article ID 103857, 2021.
[79] J.-C. He, S.-P. Zhu, C. Luo, X. Niu, and Q. Wang, "Size effect in fatigue modelling of defective materials: application of the calibrated weakest-link theory," *International Journal of Fatigue*, vol. 165, Article ID 107213, 2022.
[80] D. Liao, S.-P. Zhu, B. Keshtegar, G. Qian, and Q. Wang, "Probabilistic framework for fatigue life assessment of notched components under size effects," *International Journal of Mechanical Sciences*, vol. 181, Article ID 105685, 2020.
[81] S. Rezaei, A. Edrisi, F. Fakhri, and M. W. Khordehbinan, "Fatigue analysis of bitumen modified with composite of nano-$SiO_2$ and styrene butadiene styrene polymer," *Frattura ed Integrità Strutturale*, vol. 14, no. 53, pp. 202–209, 2020.
[82] V. Najafi Moghaddam Gilani, S. M. Hosseinian, D. Safari, and M. Bagheri Movahhed, "Investigation of the impact of deicer materials on thermodynamic parameters and its relationship with moisture susceptibility in modified asphalt mixtures by carbon nanotube," *Arabian Journal for Science and Engineering*, vol. 46, pp. 4489–4502, 2021.
[83] V. N. M. Gilani, S. M. Hosseinian, G. H. Hamedi, and D. Safari, "Presentation of predictive models for two-objective optimization of moisture and fatigue damages caused by deicers in asphalt mixtures," *Journal of Testing and Evaluation*, vol. 49, no. 6, 2021.
[84] M. Khordehbinan and M. R. Kaymanesh, "Chemical analysis and middle-low temperature functional of waste polybutadiene rubber polymer modified bitumen," *Petroleum Science and Technology*, vol. 38, no. 1, pp. 8–17, 2020.
[85] S. Rezaei, M. Khordehbinan, S.-M.-R. Fakhrefatemi, S. Ghanbari, and M. Ghanbari, "The effect of nano-$SiO_2$ and the styrene butadiene styrene polymer on the high-temperature performance of hot mix asphalt," *Petroleum Science and Technology*, vol. 35, no. 6, pp. 553–560, 2017.
[86] A. Shayesteh, E. Ghasemisalehabadi, M. W. Khordehbinan, and T. Rostami, "Finite element method in statistical analysis of flexible pavement," *Journal of Marine Science and Technology*, vol. 25, no. 2, pp. 142–152, Article ID 15, 2017.
[87] R. Babagoli, A. Ameli, S. Salari, S. M. Hosseinian, and A. Ebrahimi Moghaddam, "Investigation of the effect of combined nanosilica and iranian natural binder on the rheological behavior of mastics and performance of asphalt mixtures," *Journal of Materials in Civil Engineering*, vol. 35, no. 4, 2023.
[88] H. Ziari, B. Mojaradi, S. A. Saadatjoo, A. Amini, V. Najafi Moghaddam Gilani, and S. M. Hosseinian, "Laboratory investigation of reclaimed asphalt mixtures containing cyclogen and vacuum bottom rejuvenators," *Advances in Civil Engineering*, vol. 2023, Article ID 6223569, 11 pages, 2023.